TechnoChem

International Journal of TechnoChem Research
ISSN:2395-4248 www.technochemsai.com
Vol.01, No.03, pp135-143, 2015

Optimization of Weld Bead Geometry in Tig Welding of Copper Matrix Composite using Response Surface Methodology

Arulraj.M[1], Palani P.K[2] , Venkatesh.L[3]

[1]Department of Mechanical Engineering, Coimbatore Institute of Engineering and Technology, Coimbatore, India
[2]Department of Mechanical Engineering, Government College of Technology, Coimbatore, India
[3]Department of Mechanical Engineering, Coimbatore Institute of Engineering and Technology, Coimbatore, India

Abstract: Copper-based composite emerges as a promising material for engineering applications due to their excellent thermo physical properties coupled with better high temperature mechanical properties compared to pure copper and copper alloys. This paper deals with welding of copper matrix composite using gas tungsten arc welding. The process parameters considered in this study are arc voltage (V), welding current (I), and welding speed (S). The weld bead characteristics such as weld bead height (BH), bead width (BW), and bead penetration (BP) are the response parameters. The experiments were conducted based on Box-Behnken design with 3 factors at 3 levels. Using the results mathematical model was developed. The adequacy of the model was evaluated using analysis of variance (ANOVA). The optimum welding parameter settings were also determined using Response Surface Methodology.
Keywords: TIG welding, Copper Matrix Composite Materials, Weld Bead Geometry, Response Surface Methodology.

1. Introduction

The metal matrix composites, can exhibit unique properties if compared with traditional materials as well as potential for new applications. They wee designed with the aim to conjugate the desired characteristics of two or more materials, constitute one of the most important research fields in material science and engineering since the beginning of 60 decade. The applicability of these Copper matrix materials based on the improvement of both mechanical properties at high temperatures and wear resistance, principally when compared with conventional alloys without reinforcement.

Tungsten inert gas (TIG) welding is one of the popular metal fabrication techniques. Several welding process parameters interact in a complex manner resulting direct or indirect influence on weld bead geometry, mechanical properties and metallurgical features of the weldment as well as on the weld chemistry. Basically, TIG weld quality is strongly characterized by the weld bead geometry as shown in Figure 1.

Bead geometry variables such as bead width, bead height and penetration are greatly influenced by welding process parameters like arc voltage, welding current and welding speed.

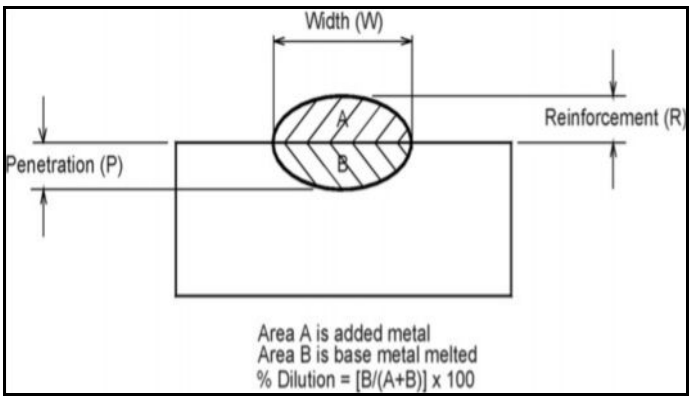

Fig.1. Weld Bead Geometry

Therefore, it is necessary to find an optimal process condition for producing desired weld quality. However, this optimization should be performed in such a way that all the objectives are fulfilled simultaneously. Such an optimization technique is called multi-response optimization.

The welding of Mo–Cu composite and 18-8 stainless steel by Tungsten Inert Gas welding process with Cr–Ni filler wires. The microstructure, element distribution, phase constituents and micro hardness of the joint were analyzed. The results indicated that austenite and ferrite phases were obtained in the weld metal. Austenite and delta ferrite structures were observed in the fusion zone near 18-8 stainless steel. The phase constituents near the fusion zone at Mo–Cu composite are Mo, Cu and c-Fe (Ni), Cu3.8Ni and the Fe–Mo compound Fe0.54Mo0.73. [1] .Tungsten inert gas (TIG) welding of SiC/6061 Al composites with and without Al–Si filler. The microstructure and fracture morphology of the joint were examined. The results indicated that adding 50 vol. % helium in shielding gas improved the arc stability, and seams with high-quality appearance were obtained when the Al–Si filler was added. [2]

The multi-response optimization of tungsten inert gas welding (TIG) process for an optimal parametric combination to yield favorable bead geometry of welded joints using the Grey relational analysis and Taguchi method. The significance of the factors on overall quality characteristics of the weldment has also been evaluated quantitatively by the analysis of variance (ANOVA) technique.

The effect of process parameters like weld current, gas flow and work piece thickness on the Bead Geometry (Front width and Back width) of the welded joint. They found that increase in weld current and gas flow results in change in bead geometry of the welded joint. Bead geometry (bead height and width) and penetration (depth and area) are important physical characteristics of weldments and several welding parameters seem to affect the bead geometry and penetration. It was observed that high arc-travel rate or low arc-power normally produced poor fusion. They found that neural network could be effectively implemented for estimating the weld bead and penetration geometric parameters [3-6]. The microstructure and properties of the oxide particle dispersion strengthened composite fabricated by internal oxidation method. The composite one to two times higher mechanical properties than those of pure copper [7]. Fabricated Mo/Cu composites with volume fractions of 55%-67% Mo by pressure die casting method. The microstructures and properties of the Mo/Cu composites were investigated [23].

From the literature survey it is observed that only very little work has been reported on the effect of TIG welding parameters on weld bead geometry of composite welds. Hence, the present study is aimed at investigating the effect of TIG welding parameter on bead geometry and optimizing process parameters to obtain optimized weld bead geometry for copper matrix composite welding.

2. Experimental Work

The composite material used in this investigation is a copper alloy reinforced with 20 vol. % Al_2O_3 particles with an average size of 10 µm. The composite materials are produced by casting method. The composite for the study are prepared as plate of 300×300 mm with 6 mm thickness. The tensile strength of parent composite is 243 MPa. For welding, the plate was made into specimens with the dimensions of 150×25×6mm. Figure 2.1 the specimen welded using TIG welding. After welding, specimens were cut into required dimensions of 50 x 10 x 6 mm, for analysis of weld bead geometry. The weld bead geometry was studied using a profile projector (Mitutoyo PJ-A3000). Weld bead specimens are shown in Fig 2.2.

Fig. 2.1. TIG Welding specimen

Fig. 2.2. Weld Bead specimen

2.1 Response Surface Methodology (RSM)

RSM is one of the optimization techniques currently in widespread use for describing the performance of the welding process and finding the optimum of the responses of interest. The objective of the present study is to establish relationships between the process parameters (inputs) and process responses (outputs) in TIG welding using RSM. The most important process parameters in TIG welding are the arc voltage (V), welding current (I) and welding speed (S). The process response characteristics considered are bead height (BH), bead width (BW) and bead penetration (BP).

2.2 Factors and Levels

The test was designed based on a three factors-three levels central box-behnken design with full replication. The TIG welding input variables are arc voltage (V), welding current (I), welding speed (S) as shown below in Table 2.1. The design matrix for conducting experiments is shown in Table 2.2. 15 experiments were conducted as per the matrix in a random manner.

Table 2.1 Parameters and levels

Parameter	Notation	Units	Factor levels		
			-1	0	1
Arc Voltage	V	Volts	25	30	35
Welding Current	I	Amps	90	120	150
Welding Speed	S	Cm/min	24	36	48

Table 2.2 Experimental design matrix

Exp.No.	Arc Voltage (V)	Welding Current (A)	Welding Speed (m/min)
1	25	90	0.36
2	35	90	0.36
3	25	150	0.36
4	35	150	0.36
5	25	120	0.24
6	35	120	0.24
7	25	120	0.48
8	35	120	0.48
9	30	90	0.24
10	30	150	0.24
11	30	90	0.48
12	30	150	0.48
13	30	120	0.36
14	30	120	0.36
15	30	120	0.36

2.3 Profile Projector

The welded plates were cross sectioned at their mid-points to obtain test specimens of 10 mm width. The specimens were prepared by the usual metallurgical polishing methods. The etchant used for obtaining the macro-structure was 0.5 ml of hydrofluoric acid plus 99.5 ml of distilled water.

The weld bead profiles were traced using an optical profile projector and the bead dimensions, (bead width, bead height, and penetration) were measured. The observed values of weld bead width, bead height, and penetration are given in Table 2.3. The profile projector Mitutoyo (PJ-A3000) as with 10 X magnification range was used.

Table 2.3. Measured values of weld bead parameters

Exp.No.	Bead Width (BW) (mm)	Bead Height (BH) (mm)	Bead Penetration (BP) (mm)
1	5.843	1.193	3.284
2	8.178	1.856	3.375
3	8.760	1.870	3.196
4	8.146	1.874	3.210
5	7.236	1.437	2.986
6	9.660	2.179	2.680
7	5.894	1.582	3.125
8	6.265	1.101	3.653
9	9.147	1.815	3.394
10	7.580	1.455	3.128
11	6.168	1.308	3.720
12	8.946	1.657	2.607
13	6.480	1.749	2.990
14	6.125	1.535	2.721
15	6.192	1.712	2.680

3. Development of Mathematical Model

Different regression functions (Linear, Linear plus square and quadratic model) are fitted to the data shown in Table 2.3 and the coefficients values are calculated using regression analysis using Minitab software.

Quadratic regression equations for bead width, bead height, bead penetration are given in Equation 3.1 to 3.3

Bead Width,

$$BW = 25.987 + 0.08715 \times (V) - 0.2324 \times (I) - 47.82 \times (S) + 0.0153 \times (V^2) + 0.0012 \times (I^2) + 42.589 \times (S^2) - 0.00491 \times (V) \times (I) - 0.855 \times (V) \times (S) + 0.3017 \times (I) \times (S) \quad \text{---------- (3.1)}$$

Bead Height,

$$BH = -6.258 + 0.279 \times (V) + 0.0158 \times (I) + 13.841 \times (S) + 0.000978 \times (V^2) + 0.000009 \times (I^2) - 7.989 \times (S^2) - 0.00109 \times (V) \times (I) - 0.509 \times (V) \times (S) + 0.0492 \times (I) \times (S) \quad \text{---------- (3.2)}$$

Bead Penetration,

$$BP = 16.1319 - 0.54312 \times (V) - 0.05784 \times (I) - 8.911 \times (S) + 0.00736 \times (V^2) + 0.000316 \times (I^2) + 9.0277 \times (S^2) - 0.000128 \times (V) \times (I) + 0.3475 \times (V) \times (S) - 0.0588 \times (I) \times (S) \quad \text{---------- (3.3)}$$

Where,

V = Arc Voltage I = Welding Current S = Welding Speed.

Table 2.4. Comparison of experimental values of bead parameters and predicted values

Exp.No.	Experiment Bead Width (mm)	Predicted Bead Width (mm)	% of Error	Experiment Bead Height (mm)	Predicted Bead Height (mm)	% of Error	Experiment Bead Penetration (mm)	Predicted Bead Penetration (mm)	% of Error
1	5.843	**5.918**	1.28	1.193	**1.332**	11.65	3.284	**3.410**	3.84
2	8.178	**8.522**	4.21	1.856	**1.893**	1.99	3.375	**3.530**	4.59
3	8.760	**8.417**	3.92	1.870	**1.832**	2.03	3.196	**3.040**	4.88
4	8.146	**8.071**	0.92	1.874	**1.735**	7.42	3.210	**3.083**	3.96
5	7.236	**6.979**	3.55	1.437	**1.307**	9.05	2.986	**3.164**	5.96
6	9.660	**9.135**	5.43	2.179	**2.151**	1.28	2.680	**2.828**	5.52
7	5.894	**6.418**	8.89	1.582	**1.609**	1.71	3.125	**2.976**	4.77
8	6.265	**6.521**	4.09	1.101	**1.230**	11.72	3.653	**3.475**	4.87
9	9.147	**9.328**	1.98	1.815	**1.805**	0.55	3.394	**3.089**	8.99
10	7.580	**8.179**	7.90	1.455	**1.621**	11.41	3.128	**3.105**	0.74
11	6.168	**5.568**	9.73	1.308	**1.141**	12.77	3.720	**3.742**	0.59
12	8.946	**8.764**	2.03	1.657	**1.666**	0.54	2.607	**2.911**	11.66
13	6.480	**6.265**	3.32	1.749	**1.665**	4.80	2.990	**2.797**	6.45
14	6.125	**6.265**	2.29	1.535	**1.665**	8.47	2.721	**2.797**	2.79
15	6.192	**6.265**	1.18	1.712	**1.665**	2.75	2.680	**2.797**	4.37

4. Result and Discussion

4.1 Analysis of Variance

The purpose of analysis of Variance is to investigate which welding parameters significantly affect the performance characteristic. This is accomplished by separating the total variability of the grey relational grades, which is measured by the sum of the squared deviations from the total mean of the grey relational grade, into contributions by each welding parameters and the error. In addition, the F test was used to determine which welding parameters have a significant effect on the performance characteristic. Usually, the change of the welding parameter has a significant effect on the performance characteristic when the F value is large. ANOVA results for weld bead geometry are shown in Table 4.1, 4.2 & 4.3.

Table 4.1. Analysis of Variance for Bead Width

Source	DF	SS	MS	F	F (3,2,0.05)	Contribution (%)
Regression Model	9	23.254	2.583	7.24	19.16	92.90
Linear	3	9.686	3.228	9.04	19.16	38.70
Square	3	5.620	1.873	5.25	19.16	22.40
Interaction	3	7.947	2.649	7.42	19.16	31.73
Residual Error	5	1.785	0.357			
Lack Of Fit	3	1.714	0.571	16.06	19.16	7.10
Pure Error	2	0.0712	0.0355			
Total	14	25.040				100

S = 0.5976 R-Sq = 92.9%, R-Sq (adj) = 80%

Table 4.2. Analysis of Variance for Bead Height

Source	DF	SS	MS	F	F (3,2,0.05)	Contribution (%)
Regression Model	9	1.019	0.113	3.58	19.16	86.60
Linear	3	0.357	0.119	3.76	19.16	30.30
Square	3	0.053	0.017	0.57	19.16	4.50
Interaction	3	0.608	0.202	6.40	19.16	51.60
Residual Error	5	0.158	0.031			
Lack Of Fit	3	0.132	0.044	3.37	19.16	13.40
Pure Error	2	0.026	0.013			
Total	14	1.178				100

S = 0.1780 R-Sq = 86.6%, R-Sq (adj) = 72.4%

Table 4.3. Analysis of Variance for Bead Penetration

Source	DF	SS	MS	F	F (3,2,0.05)	Contribution (%)
Regression Model	9	1.238	0.137	1.60	19.16	74.20
Linear	3	0.451	0.150	1.75	19.16	27.02
Square	3	0.432	0.144	1.68	19.16	25.88
Interaction	3	0.354	0.118	1.37	19.16	21.22
Residual Error	5	0.430	0.086			
Lack Of Fit	3	0.373	0.124	4.39	19.16	25.80
Pure Error	2	0.056	0.028			
Total	14	1.669				100

S = 0.2934 R-Sq = 74.2%, R-Sq (adj) = 62%

Result of the ANOVA indicates that the welding speed is the most effective parameter on the responses under the multi criteria optimization (higher penetration, lower bead width, bead height). The percent contributions of other parameters are arc voltage and current not more effective when compare to welding speed.

4.2 Effect of Welding Parameters on Bead Width

The main effects of the weld parameters such as voltage, current, and welding current on bead width as shown in Fig. 4.1. From the graphs it is observed that bead width increased with increasing voltage, whereas, it decrease to a minimum value and further increase in current it starts increasing. The bead width decreases with the increase in welding speed.

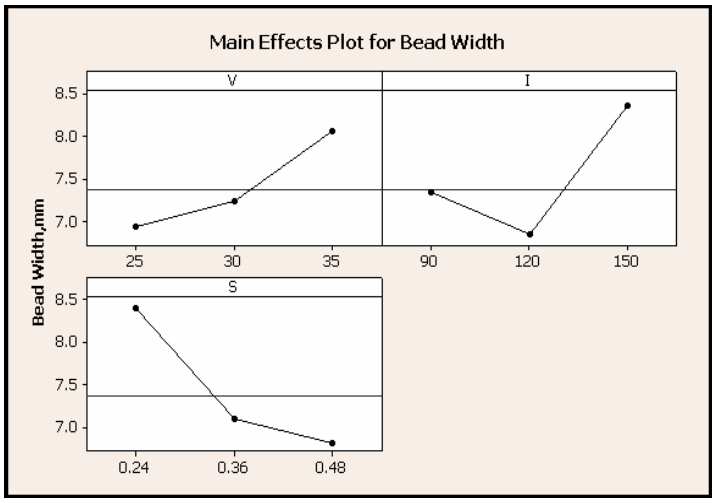

Fig. 4.1. Main effect plot for bead width

4.3 Effect of Welding Parameters on Bead Height

The main effects of the weld parameters such as voltage, current, and welding current on bead height as shown in Fig. 4.2. From the graphs it is observed that bead height increased with increasing voltage, whereas, it decrease to a minimum value and further increase in current it starts increasing. The bead height decreases with the increase in welding speed.

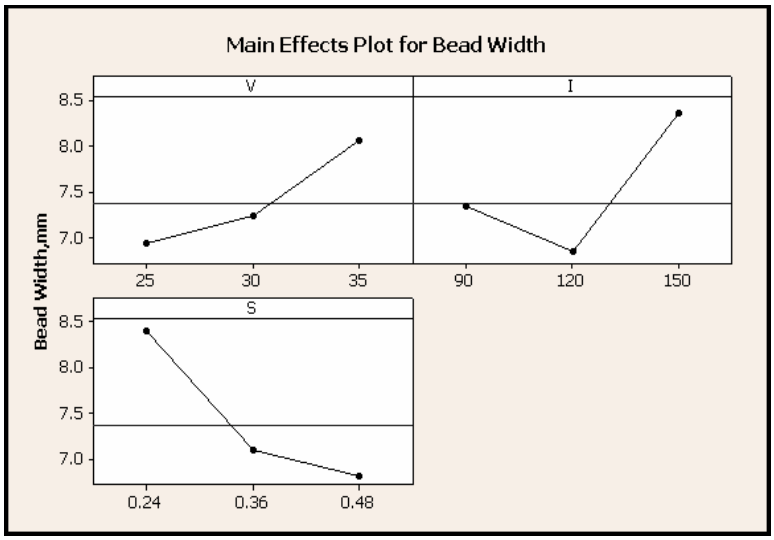

Fig. 4.2. Main effect plot for bead height

4.4 Effect of Welding Parameters on Bead Penetration

The main effects of the weld parameters such as voltage, current, and welding current on bead height as shown in Fig. 4.3. From the graphs it is observed that bead penetration decreased with increasing voltage and current whereas, it decrease to a minimum value and further increase. The bead penetration increases with the increase in welding speed.

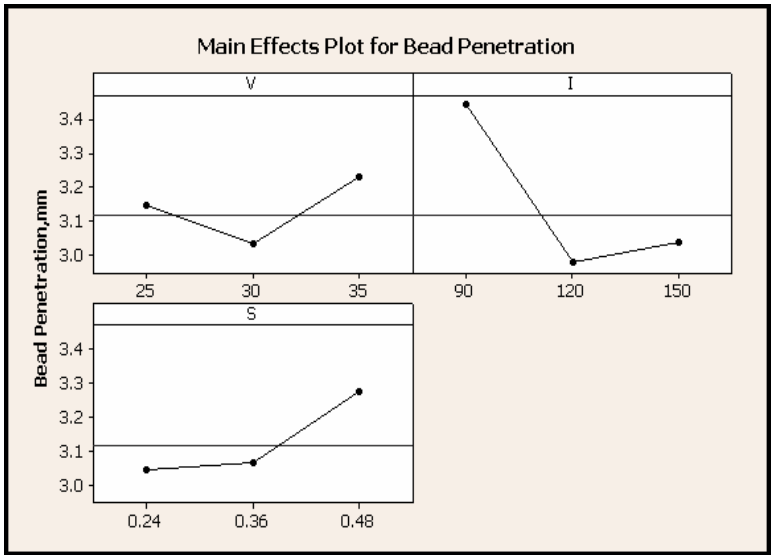

Fig.4.3. Main effect plot for bead penetration

4.5 Optimum Parameter:

From the above design of experiment results using MINITAB software and the experimental values of the response (Bead geometry characteristics) the optimized parameter can be shown in Figure 4.4.

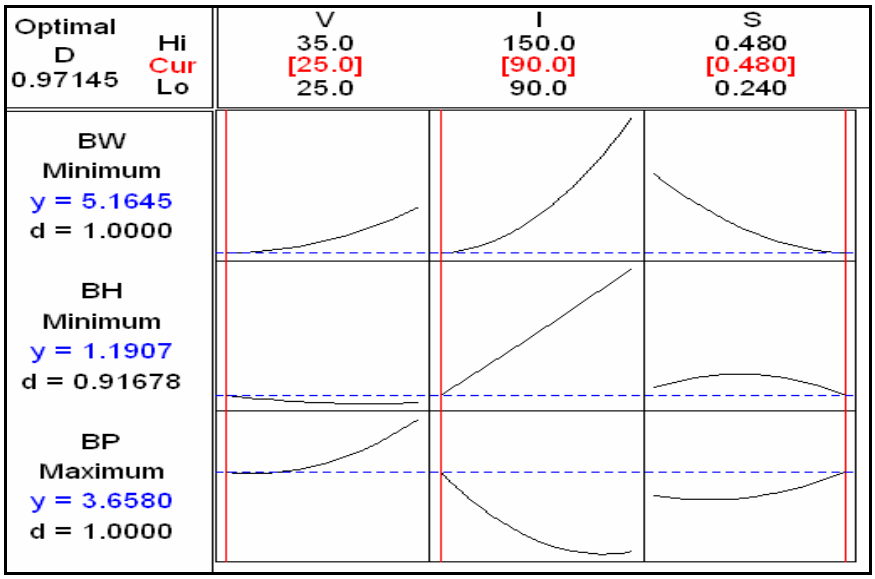

Fig.4.4. Optimum Parameters

5. Conclusion

Response surface methodology (RSM) can be effectively used to find optimum condition for TIG welding of copper matrix composite. Essential requirements for all types of welding are deep penetration, lower bead width and bead height for reducing weld metal consumption. From the experimental results, mathematical models were developed to express in terms of arc voltage, welding current, welding speed. The adequacy of the model was evaluated using analysis of variance (ANOVA) technique. Optimization using Response Surface Methodology has also been done to determine optimum process parameters to obtain desirable weld bead geometry.

The optimum condition of process parameters in found to be Arc Voltage = 25 Volts, Welding Current = 90 Amps, Welding Speed = 0.48 m/min. and the corresponding weld bead parameters are found to be bead width = 5.1645 mm, bead height =1.1907 mm, penetration = 3.6580 mm.

6. References

1. Jiang Qjnglei, Li Yajiang (2010), Microstructure characteristics in TIG welded joint of Mo-Cu composite and 18-8 stainless steel Int. Journal of Refractory Metals & Hard Materials 28, pp. 429-433
2. Wang Xi-he, Niu Ji-tai (2009) Investigation on TIG welding of SICp-reinforced aluminium-matrix composite using mixed shielding gas and Al-Si filler Materials science and Engineering A 499, pp. 106-110
3. Ugur Esme , Melih Bayramoglu (2009) Optimization of weld bead geometyin TIG welding process using grey relation analysis and taguchi method Original scientific article MTAEC9 ,43(3) , pp. 143-149
4. A.Kokangul,M.Bayramoglu (2009) Mathematical modeling for prediction and optimization of TIG welding pool geometry METABK 48(2) , pp. 109-112
5. Manoj Singla, Dharinder Singh (2010) Parametric optimization of gas metal arc welding processes bu using factorial design approach Journal of Minerals & Materials Characterization & Engineering, Vol.9, No.4, pp. 353-363
6. P.K.Palani, N.Murugan (2006) Selection of parameters of pulsed current gas metal arc welding Journal of Materia; Processing Technology, Vol.No. 172, pp. 1-10
7. Jianjun WU, Guobin LI (1999) Copper Matrix Composites Reinforced with Nanometer Alumina Particle Journal of Materials science and Technology, Vol.15 No.2, pp. 143-146
8. JIANG Long-tao, WU Gao-hui (2007) Fabrication and characterization of high dense Mo/Cu composites for electronic packaging applications Trans.Nonferrous Met.Soc. China 17, pp. 580-583
9. D.C. Montgomery, G.C. Runger, (1999) Applied Statistics and Probability for Engineers, second ed., John Wiley & Sons Inc., New York.

10. J.B. Fogagnolo et al (2000) Aluminium AA6061matrix composite reinforced with nitrides particles produced by mechanical alloying, in: Proceedings of the PM 2000 – Powder Metallurgy World Conference and Exhibition, Kyoto, Japan, pp. 1045–1048
11. M. Adamiak, J.B. Fogagnolo et al (2001) AA6061/(Ti3Al)p composite powder obtained by mechanical milling, in: Proceedings of the 10th International Conference on Achievements in Mechanical & Materials Engineering, Zakopane, Poland, pp. 15–18
12. B.J.M. Aikin, T.H. Courtney (1992) The kinetics of composite particle formation during mechanical alloying, Metall. Trans. A 24, pp. 647
13. Amirkhanlou S. (2010) Fabrication and characterization of Al356/SiCp semi-solid composite produced by injection of SiCp containing composite powders. MSc thesis, Isfahan University of Technology
14. Jamaati R, Toroghinejad MR, Najafizadeh A. (2010) An alternative method of processing MMCs by CAR process. Mater Sci Eng A,pp. 2720–4
15. Seyed Reihani SM. (2006) Processing of squeeze cast Al6061–30vol%SiC composites and their characterization. Mater Des: pp. 216–22
16. Jamaati R, Toroghinejad MR. (2010) High-strength and highly-uniform composite produced by anodizing and accumulative roll bonding processes. Mater Des, 31: pp. 4816–22
17. Jamaati R, Toroghinejad MR. (2010) Manufacturing of high-strength aluminum/ alumina composite by accumulative roll bonding. Mater Sci Eng A, 527: pp. 4146–51
18. Burke MA, Lessmann GG. Method for laser beam welding metal matrix composite components. US Pat. No. 4803334
19. Uzun H.(2007) Friction stir welding of SiC particulate reinforced AA2124 aluminium alloy matrix composite. Mater Des, 28: pp. 1440–1446
20. Huang JH, Dong YL, Wan Y, Zhao XK, Zhang H. (2007) Investigation on reactive diffusion bonding of SiCp/6063 MMC by using mixed powders as interlayers. J Mater Process Technol, 190: pp. 312–316
21. Shirzadi AA, Wallach ER. (1997) New approaches for transient liquid phase diffusion bonding of aluminum based metal matrix composites. Mater Sci Technol, 13: pp. 135–42
22. Zhou Y, North TH. (1997) Counteracting particulate segregation during transient liquid-phase bonding of MMC–MMC and Al2O3–MMC joints. J Mater Sci ,32:pp. 5571–5576
23. Chen RF, Zuo DW, Wang M. (2006) Improvement of joint strength of SiCp/Al metal matrix composite in transient liquid phase bonding using Cu/Ni/Cu film interlayer. J Mater Sci Technol, 22: pp. 291-295
24. Ureña A, Gil L, Escriche E, et al (2006) High temperature soldering of SiC particulate aluminum matrix composites (series 2000) using Zn–Al filler alloys. Sci Technol Weld J 6: pp.1–11

*****